

Contents

9.	A Minimal Model of City Traffic: Chaos, Critical Behavior and Control	267
1	Introduction	267
2	The Microscopic Model	268
2.1	Fuel consumption	270
3	Zero Phase Control Strategy: Resonant Behavior	271
3.1	Existence of a chaotic regime	272
3.2	Resonance and control	273
4	Green Wave Control Strategy	275
5	Transient Behavior	281
6	Parrondo-like Games for Controlling	285
7	Conclusion	287
	References	289

Chapter 9

A MINIMAL MODEL OF CITY TRAFFIC: CHAOS, CRITICAL BEHAVIOR AND CONTROL

J. A. Valdivia, B. A. Toledo, V. Muñoz and J. Rogan

1. Introduction

The complex behavior displayed in traffic patterns is an interesting field of physics that have been attracting some attention for several decades [7], in particular for their statistical [10, 19] and dynamical [9, 24] properties. There are a number references on traffic jams, chaotic traffic flows, bus-route problems, pedestrian flows, etc. [6, 12–14, 16, 17]. In particular, the development of complex behavior in traffic flows determines, in a certain way, the efficiency of the transportation infrastructure of a city, region, or country. In this context, traffic flows, with and without passing, have been studied extensively in the literature [1, 15], e.g., cellular automaton models, mean-field theories which test the microscopic evolution, hydrodynamic models which approach collective behavior, etc. [11, 20].

In this chapter, we will formulate “a minimal model of city traffic”, where we will follow the behavior of cars moving through a sequence of street light signals, and discuss different control schemes. In this model, the street lengths can be fixed or variable and the control is applied to the frequency and relative phase of the traffic lights.

It is worth noticing that the timing of traffic lights must be close to the characteristic traveling time e.g., including car interaction and so on between signals, since longer or shorter timing will slow down the car mean speed, and may contribute to jam the road [18]. This suggests that resonant conditions may lead to efficient traffic systems, but more importantly, resonance and control are related. Moreover, it will be shown that around resonance, for our model, dynamical variables follow certain power laws.

Such power laws resemble scaling relations near second order phase transitions, and in view of this analogy we refer to them as critical behavior. We plan to characterize this criticality and derive the critical behavior close to the resonance in terms of traveling time, velocity, and fuel consumption. In particular, we will discuss in detail a common control strategy used in cities, the “green wave” [3], in which a green signal is made to propagate with velocity v_{wave} the applicability to other synchronization strategies will be discussed below.

This particular control method tends to produce clusters of vehicles, and due to this high correlation, a precise knowledge of the leading car can provide us with information about the cluster itself. Therefore, as long as the leading car represents the behavior of the cluster to which it belongs (this occurs for low noise conditions), we can describe with a single car model some common states in traffic behaviors involving clusters of vehicles [11]. Because of this, we will limit ourselves in this chapter to study a single car moving through a sequence of traffic lights [22, 23].

Hence, within this model, we will analyze three control strategies: (a) the zero phase strategy, (b) the green wave strategy, and (c) a Parrondo-like strategy that considers the transients.

2. The Microscopic Model

The aim of our approach is to follow the details of one vehicle moving through a sequence of traffic lights in one dimension. The separation between the n^{th} and $(n + 1)^{\text{th}}$ traffic light is L_n . The n^{th} light is green if $\sin(\omega_n t + \phi_n) > 0$ and red otherwise, where ω_n is the frequency of the n^{th} traffic light, and ϕ_n is the phase shift. Note that these two parameters are important if we were trying to control the traffic flow.

A car in this sequence of traffic lights can have (a) an acceleration a_+ until its velocity reaches the cruising speed v_{\max} , (b) a constant speed v_{\max} with zero acceleration, or (c) a negative acceleration $-a_-$ until it stops, hence

$$\frac{dv}{dt} = \begin{cases} a_+ \theta(v_{\max} - v) , & \text{accelerate,} \\ -a_- \theta(v) , & \text{brakes,} \end{cases} \quad (1)$$

where $\theta(x)$ is the Heaviside step function.

As the car approaches the n^{th} traffic light with velocity v the driver must make a decision, to step on the brakes or not, at the distance (the last stopping point) $v^2/2a_-$ depending on the sign of $\sin(\omega_n t + \phi_n)$. Note that if

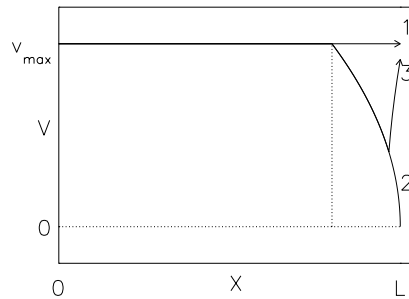


Fig. 1. The possible situations at the decision point, namely, (1) continuing, (2) braking to stop at $x = L$ before the light turns green again, and (3) braking and accelerating again as the light turns green before stopping completely.

$(v_{\max}^2/2a_+) + (v_{\max}^2/2a_-) < L_n$, then $v = v_{\max}$ and the car reaches cruising speed before reaching the decision point. Also in general it makes sense that $(2\pi/\omega_n) > (v_{\max}/a_-), (v_{\max}/a_+)$ so that the traffic light does not change too fast from red to green. Of course as the vehicle brakes two things can happen, the car can stop completely and wait until the light turns on again, or it can start accelerating before it stops completely if the light changes. Here we start observing the discontinuous nature of the model.

The type of trajectories between two traffic lights are described in Fig. 1, which clearly shows the typical kinematics associated to this model.

It is interesting to mention that this simplified model may still be relevant in the case of many cars going through the traffic light sequence, but with the effective parameters depending on the density of interacting cars. For example, you may have observed while driving through a city that the effective averaged acceleration seems to depend on the number of cars waiting at the traffic light. Similarly, the averaged effective cruising speed also seems to depend on the density of cars going through the sequence of traffic lights.

We now study the situation of a car traveling through a sequence of N traffic lights, which in essence assumes a city with regular city blocks. We expect that iterating this map may reveal interesting information about the behavior of traffic flow in a city, even with this simplified model. The car enters the sequence of traffic lights with velocity v_0 and time t_0 . The set of rules described above determine a 2-D map $M(v_n, t_n)$ that evolves the state (t_n, v_n) at the n^{th} traffic light to state (t_{n+1}, v_{n+1}) at the $(n + 1)^{\text{th}}$ traffic light. This map is constructed explicitly in the appendix.

2.1. Fuel consumption

Even though travel time and velocity are good characterizations of the efficiency of a road system, fuel consumption is also of interest to drivers. In general, fuel efficiency will improve if the number of times the car stops is reduced, but it depends on the specific sequence of brakings and accelerations, and thus on the initial conditions. However, general conclusions can be obtained by studying the evolution of the attractor solution.

To account for fuel consumption, we need to study the main sources of dissipation in the car's motion. Fuel consumption is proportional to the mechanical energy produced by the engine, given by $\int_{t_0}^{t_f} Fv dt$, where t_0 and t_f are the initial and final times for the complete journey, and F is the forward force or thrust. Besides the engine thrust, we have the rolling friction F_r which opposes the motion, and F_d , where we include other resisting forces such as aerodynamic drag. Therefore, if m is the car mass, the following equation holds:

$$F = ma_+ + F_r + F_d . \quad (2)$$

An analogous equation for the braking state is not necessary, as we assume that the forward force provided by the engine is zero while braking. Let us consider each term in Eq. (2) separately. The car acceleration is a_+ , as given by Eq. (1), and the total injection of energy due to the acceleration from rest to v_{\max} is $mv_{\max}^2/2$. Each time the car stops, this energy is wasted, so this term represents the effect of the driver's behavior on fuel consumption. The rolling friction is estimated as $F_r = \mu mg$, where mg is the weight of the car and μ is the coefficient of rolling friction [5]. Rolling dissipation is thus given by $\int F_r v dt \sim F_r L$, which is a function of the distance between traffic lights. Both sources of energy losses can be compared through the dimensionless number $f_r \equiv 2F_r L / mv_{\max}^2 \sim 2\mu g L / v_{\max}^2$ which is $f_r \sim 0.2$ for a car traveling at 50 km/h between lights 200 m apart and a rolling coefficient of $\mu = 0.01$ [21].

Finally, the force F_d is a function of the car velocity. Most of the fuel consumption in a non-stop journey is due to the rolling and drag forces, since accelerations are minimal. However, if the car passes through a sequence of traffic lights, it moves at lower speeds, and then drag is less important than rolling friction. Hence, we neglect drag dissipation in our analysis. We also neglect other dissipative sources such as the energy needed to keep the motor running (in particular, the energy wasted while standing at the traffic light) and the energy lost due to internal frictions in the car mechanisms [4].

Thus, under city traffic conditions, total fuel consumption can be estimated as

$$C = \int_{t_0}^{t_f} Fv dt = ma_+L_+ + F_r(L_+ + L_0), \quad (3)$$

where L_+ is the portion of the traveling length in which the driver was accelerating and L_0 is the distance traveled at constant speed.

For now, we will concentrate on studying the dynamics for a given value of v_{\max} . Note that this parameter is very relevant in actual city situations since different drivers are willing to reach different values of v_{\max} , and traffic light control strategies, achieved through ω_n and ϕ_n , will be very sensitive to its distribution. Furthermore, if we assume that the traffic parameters are, to first order, functions of the density or number of cars, then control strategies must take this into account specially during traffic jams.

3. Zero Phase Control Strategy: Resonant Behavior

In Ref. [23], a specific strategy of traffic light synchronization was considered, namely, all lights have equal phase $\phi_n = 0$. This synchronization, which we consider now, makes sense only if $L_n = L$. Later on we will relax this restriction when we apply other control strategies. Note that we could consider different $L_n = L + \Delta L_n$ values and different frequencies $\omega_n = \omega + \Delta\omega_n$ values as induced phase shifts $\Delta\phi_n = \Delta L_n/v_{\max}$ and $\Delta\phi_n = \Delta\omega_n L/v_{\max}$ respectively. That is why we concentrate for simplicity on the situation $L_n = L$, and $\omega_n = \omega$.

If the period of the signals, $2\pi/\omega$, is equal to the cruising time, T_c , after a short transient (passing a few traffic lights), the car will arrive at each successive decision point when the light's phase is the same. It is important to note that such resonance between the car motion and traffic signals corresponds to a very narrow region of parameters (see the period-1 orbit in Fig. 2). Thus, the interesting regime for controlling traffic situations corresponds to a narrow region around the condition $2\pi/\omega = T_c$. Introducing the dimensionless quantity $\bar{\Omega} = \omega T_c/2\pi$, resonance occurs at $\bar{\Omega} = 1$.

Figure 2 gives the bifurcation diagram of a car starting from rest at the first traffic light. For a given frequency of the traffic lights, characterized by $\bar{\Omega}$, the normalized speed v_n/v_{\max} and time travel between traffic lights $(t_{n+1} - t_n)/T_c$ at the n^{th} light is plotted. A transient of 500 time steps has been removed. This is too large a number of traffic lights to be relevant in real traffic situations, but it is necessary to reach the attractor for all the

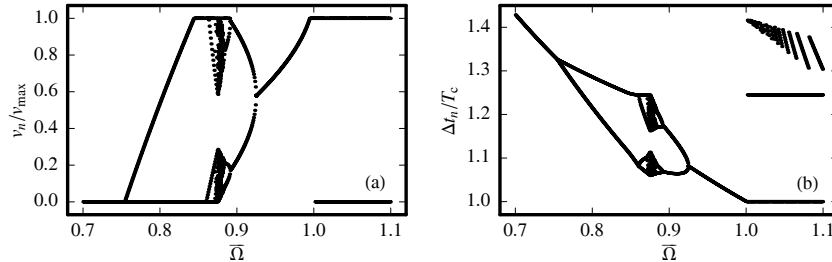


Fig. 2. Bifurcation diagram for the normalized (a) speed at the traffic lights and (b) time travel between traffic lights, versus normalized frequency $\bar{\Omega}$, for $a_+ = 2 \text{ m/s}^2$, $a_- = 6 \text{ m/s}^2$, $v_{\max} = 14 \text{ m/s}$, and $L = 200 \text{ m}$. A transient of 500 time steps has been removed.

initial conditions plotted (specially in the region very close to the period-doubling bifurcation, where convergence is particularly slow). However, we should point out that most of the initial conditions converge to the attractor in as few as 5–20 traffic lights.

It is important to notice that even in this model there is already an interesting nontrivial behavior in the range $0.75 < \bar{\Omega} < 1$ as displayed in Fig. 2, where a necessary condition for complexity emerges even from the dynamics of a single car. It includes a period doubling bifurcation transition to chaos, where the Lyapunov exponent is estimated in Toledo et al. [2004] for a similar situation. It is interesting to note that this chaotic behavior is produced by the finite accelerating and braking capabilities of the cars, and is thus independent of the interactions between cars. This is one of the reasons for which this model could be an interesting starting point for a first principles approach to traffic in cities.

3.1. Existence of a chaotic regime

The bifurcation diagram of Fig. 2 suggests a period doubling bifurcation to chaos as we increase $\bar{\Omega}$. A crisis occurs as the chaotic attractor collides with one of the velocity thresholds, producing an inverse period double bifurcation. If we zoom into one of the frequency ranges where the map displays complex behavior, as shown in Fig. 3(a), we find an intricate structure of steady and chaotic behavior.

Estimating the relevance of this chaotic behavior and its sensitivity to perturbation and noise, may be of importance in control strategies. In this sense a finite amplitude Lyapunov exponent can be estimated [2]. Let us take a trajectory in the attractor that starts from (u_0, τ_0) and an initially

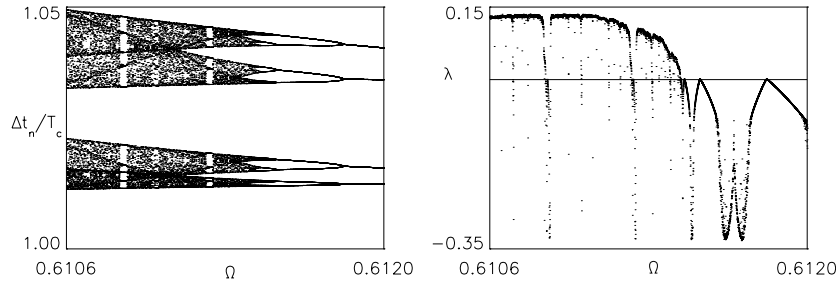


Fig. 3. The bifurcation diagram, (a) zoom for Fig. 4(b), and (b) the associated Lyapunov exponent.

perturbed trajectory that starts from $(u_0, \tau_0 + \delta_0)$, with for example $\delta_0 = 10^{-7}$. The error is iterated n times producing δ_n . Care must be taken to include only the scaling region where

$$\delta_n \sim \delta_0 e^{\lambda n}.$$

Given an initial condition over the attractor an exponent can be estimated by a fitting procedure in the scaling region. Of course, the discontinuous nature of the map complicates this calculation, where for example, both trajectories can reach the same state in one step, yielding $\lambda = -\infty$.

But a final Lyapunov exponent can still be constructed by averaging many initial conditions over the attractor, as shown in Fig. 3(b).

3.2. Resonance and control

Intuitively, and from Fig. 2, at $\bar{\Omega} = 1$ the car motion is in resonance with the traffic lights and the traveling time between two given traffic signals is minimized. For $\bar{\Omega} > 1$ (increasing ω), there are a number of resonances, separated by $\Delta\omega = 2\pi/T_c$. Figure 4 displays the average normalized speed $\langle v \rangle / v_{\max}$ (total distance traveled divided by total time elapsed) as a function of frequency. Successive resonant points are found at $\bar{\Omega} = \ell$, where ℓ is a positive integer. We will see below that these resonances display critical behavior. On the other hand for $\bar{\Omega} < 1$ there are situations in which the car covers a distance qL , with q a positive integer, with cruising speed for half the period of the traffic lights, and then is stopped for the other half of the period. In these cases $\bar{\Omega} = 1/q$ and the average normalized speed is $\langle v \rangle / v_{\max} = 1/2$ as shown in Fig. 4. Since for a reasonable city $L \approx 200$ m and $v_{\max} \approx 50$ km/h, the traffic light period of the first

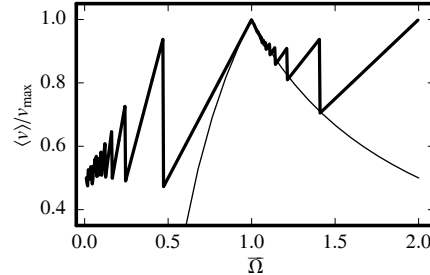


Fig. 4. Resonant tongues showing the average speed (total distance traveled divided by total time elapsed) as a function of the forcing frequency $\bar{\Omega}$. The thin line corresponds to the scaling relation Eq. (23). A transient of 500 time steps has been removed.

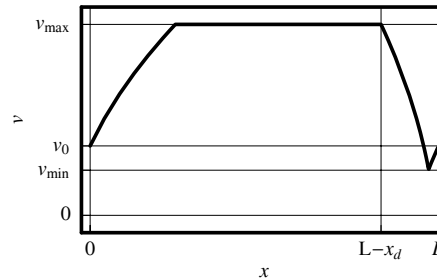


Fig. 5. Speed versus distance for the period-1 attractor below resonance ($\bar{\Omega} < 1$). The car starts at the first traffic light with velocity v_0 , accelerates until reaching velocity v_{\max} , and arrives at the decision point $L - x_d$ when the next traffic light is red, so it brakes. When the velocity is a certain minimum value v_{\min} , the sign turns green, and the car accelerates again, passing the traffic light with the initial speed v_0 .

resonance $P = 2\pi/\omega \approx 14$ s is a little unreasonable, an attempt to control the system using this parameter alone seems impractical, however, exploring this dynamics could allow us to derive more practical control schemes.

In the vicinity of the resonance $\bar{\Omega} \approx 1$, two different dynamics arise depending on the sign of $\bar{\Omega} - 1$. For simplicity, let us consider a car starting at the first traffic light when it changes from red to green, *i.e.*, when the green window begins. If $\bar{\Omega} < 1$, the car will be delayed with respect to the traffic lights, and will reach the second one when it is red, so it will be forced to brake. However, if the delay is small, the traffic light will turn green before the car gets to a full stop, so the car will accelerate again (see Fig. 5), reaching the next traffic light with non-zero velocity. This causes the period-1 orbit below the resonance $\bar{\Omega} = 1$ of Fig. 2.

The situation for $\bar{\Omega} > 1$ is very different. The car reaches the second light a time δt after it has turned green, and this delay increases with each traffic light until it is eventually forced to stop. Thus, for $\bar{\Omega} > 1$, the car moves at maximum speed almost always, except for a stop every p traffic lights, leading to the attractor seen above the resonance in Fig. 2.

To estimate p , we note that the driver arrives at the next signal a small time $\delta t = T_c - 2\pi/\omega > 0$ after the signal turns green, then with a delay $2\delta t$ at the third light, and so on. The journey will continue until the green window is exhausted. The total number of signals, p , that the driver will cross without stopping is given by $p\delta t \approx \pi/\omega$, which leads to

$$p \approx \frac{1}{2} \frac{1}{\bar{\Omega} - 1}. \quad (4)$$

Equation (4) is very interesting, because it also suggests that there is a critical behavior of traffic variables around resonance. However, resonance itself is not a robust feature for $\phi_n = 0$, as it is not independent of the geometry of the road, which is important, because in real situations the distance between traffic lights is not constant, being impossible to maintain resonance while traveling at constant speed.

Fortunately, the opposite is true for another kind of traffic light synchronization strategy, the “green wave”, which we now consider.

4. Green Wave Control Strategy

A common strategy for traffic light synchronization is the “green wave”, where a green color signal is moved with a speed v_{wave} , so that the color at the n^{th} traffic light, located at a position x_n along the road, is given by $\sin \omega(t - x_n/v_{\text{wave}})$, where ω is the frequency of the traffic light. This implies that $\phi_n = -\sum_{m=1}^n L_m \omega / v_{\text{wave}}$. The case $\phi_n = 0$ analyzed in Sec. 3 is equivalent to the green wave case with $v_{\text{wave}} \rightarrow \infty$.

In Fig. 6 we plot the bifurcation diagram with $\alpha = v_{\text{max}}/v_{\text{wave}}$ of a car starting from rest for a road with constant distance between traffic signals $L_n = L = 200$ m, constant frequency $\omega = 2\pi/60$ s⁻¹, accelerations $a_+ = 2$ m/s² and $a_- = 6$ m/s², and $v_{\text{wave}} = 14$ m/s. These parameters are reasonable for an actual road, corresponding to a change of lights every 30 s, and a green wave synchronized with cars moving at 50 km/h. The car will follow a complex path unless the velocity of the car coincides with the wave velocity, *i.e.*, a resonance. Under this condition, the driver will never be stopped. However, resonance is rather fragile, as observed in Fig. 6, hence the dynamics must be observed near the resonant condition $\alpha \sim 1$.

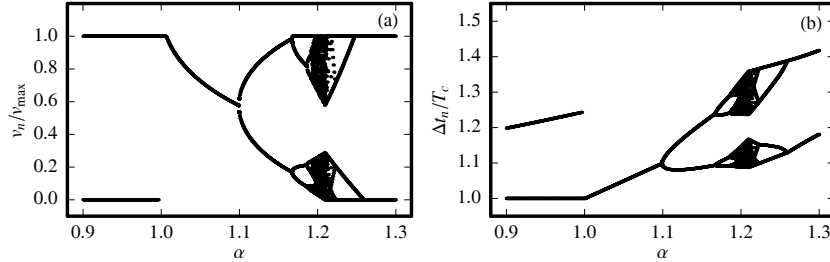


Fig. 6. Bifurcation diagram for (a) normalized speed and (b) normalized time travel between traffic lights, versus α , for $a_+ = 2 \text{ m/s}^2$, $a_- = 6 \text{ m/s}^2$, $v_{\text{wave}} = 14 \text{ m/s}$, $\omega = 2\pi/60 \text{ s}^{-1}$, $L = 200 \text{ m}$. The transient has been removed.

The bifurcation diagram in Fig. 6 is very similar to Fig. 2, but reflected horizontally. Thus, it is above resonance, $\alpha > 1$, that a period-1 solution exists, where the car follows a trajectory like Fig. 5, and below resonance the car crosses a certain number p of lights before being stopped. An approximate expression for p can be obtained for the green wave, using similar arguments to those used to derive Eq. (4).

Let us consider the number of traffic lights the car can pass without braking. In the green wave case, close to resonance, we consider a small perturbation $\delta v = v_{\text{wave}} - v_{\text{max}} > 0$. In the optimal case, the driver starts at one extreme of the green semi-period just when the signal changes from green to red, so that at the next signal the driver arrives a time $\delta t = L/v_{\text{max}} - L/v_{\text{wave}}$ before the signal turns red. The journey will continue until the green window is exhausted. The total number of signals, p , that the driver will cross without stopping is given by $p \delta t = \pi/\omega$, or

$$p \approx \frac{\lambda/L}{2} \frac{\alpha}{1 - \alpha}, \tag{5}$$

where $\lambda = v_{\text{wave}} \cdot 2\pi/\omega$. Criticality is, once more, explicit. However, unlike the case $\phi_n = 0$, resonance for the green wave holds even if the distance between traffic lights is not constant, in which case $\phi_n = -\sum_{m=1}^n L_m \omega/v_{\text{wave}}$. Regarding the quantity p we can do even a little more. If we take advantage of the periodic nature of the solution in the asymptotic regime we can derive the following expression, exact to second order for $\alpha \in (0.67, 1)$,

$$p = \left\lceil (\pi - \xi) \sqrt{\frac{6}{15 - 16 \cos\left(\frac{2\pi L}{\lambda \alpha}\right) + \cos\left(\frac{4\pi L}{\lambda \alpha}\right)}} \right\rceil, \tag{6}$$

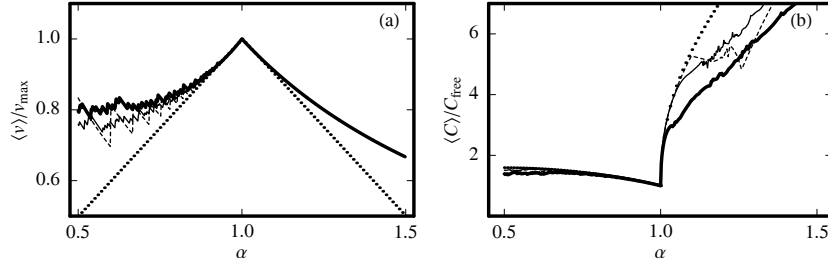


Fig. 7. (a) Resonant tongue showing the average speed (total distance traveled after crossing n signals, divided by time elapsed) as a function of the parameter α . The thin line corresponds to random street length, the thick line corresponds to the Alameda Avenue, the dashed line corresponds to constant street length, and the dotted line corresponds to the scaling laws derived in the text, (b) The corresponding average fuel consumption, normalized to the free consumption $C_{\text{free}} = nF_r L$.

where

$$\xi = \frac{2\pi v_{\max}}{\lambda\alpha} \left[\frac{L}{v_{\max}} + \frac{v_{\max}}{2} \left(\frac{1}{a_+} - \frac{1}{a_-} \right) \right] \bmod 2\pi,$$

and the function $[x]$ is the ceiling function, the function that returns the the closest upper integer of x .

An interesting example of this independence of geometry for the behavior near resonance is shown in Fig. 7(a) for the average speed after traveling a large number of traffic lights as a function of $\alpha = v_{\max}/v_{\text{wave}}$. Three cases are compared: (i) a street where distance between traffic lights $L_n = L = 200$ m is constant; (ii) a street with a random distribution of distances $L_n = L + \Delta L_n$, where $\Delta L_n/L$ is a uniform random number in the interval $[-0.5, 0.5]$; and (iii) a real street, namely, the longest city street in Chile (the Avenida del Libertador Bernardo O'Higgins, also known as Alameda Avenue; its precise geometry can be obtained from the Chilean Military Geographic Institute at <http://www.igm.cl/>). All curves are identical at resonance. The same is true for the average time between traffic lights. This suggests that behavior near resonance for the green wave, at $\alpha = 1$, is indeed universal, regardless of the detailed geometry of the road. Moreover, it will be shown that near resonance, traffic variables behave according to scaling laws. Thus, Fig. 7 shows the universality of this critical behavior. The figure also shows how the efficiency of the strategy degrades as the effective speed of the cars gets away from v_{wave} .

Based on Eq. (5), it is now easy to obtain scaling laws for the traffic variables (time, velocity, fuel consumption). At $\alpha = 1$, the system is at

resonance, so that the average travel time $\langle t \rangle$ is equal to the time of “free” travel, when no red lights are found, $T_{\text{free}} \equiv nL/v_{\text{max}}$, where n is the number of passed traffic lights. Average velocity is equal to the corresponding maximum or free velocity $\langle v \rangle = V_{\text{free}} \equiv v_{\text{max}}$. Below resonance these relations change because, if $\alpha < 1$, the car is forced to stop at some point. Since π/ω is the time the red light window lasts, the car is at rest a time $\approx k\pi/\omega$ with k as the number of times the driver brakes. Then the average travel time is

$$\langle t \rangle = T_{\text{free}} + \frac{k\pi}{\omega}. \quad (7)$$

The average velocity in the same run is

$$\langle v \rangle \sim \frac{nL}{\langle t \rangle}. \quad (8)$$

Fuel consumption at resonance, on the other hand, is $\langle C \rangle = C_{\text{free}} \equiv nF_r L$. Below resonance fuel consumption can be estimated by observing that the car stops k times when it covers a distance nL at cruising speed, hence $\langle C \rangle \sim F_r nL + kmV_{\text{free}}^2/2$, which is the total work done by F_r plus the energy wasted in each stop, thus

$$\langle C \rangle \sim C_{\text{free}} \left(1 + \frac{mkV_{\text{free}}^2/2}{nF_r L} \right). \quad (9)$$

Equations (7) to (9) can be written as

$$\begin{aligned} \frac{\langle t \rangle - T_{\text{free}}}{T_{\text{free}}} &\sim \frac{\lambda}{2L} \frac{k}{n} \alpha, \\ \frac{\langle v \rangle - V_{\text{free}}}{V_{\text{free}}} &\sim -\frac{\lambda}{2L} \frac{k}{n} \alpha, \\ \frac{\langle C \rangle - C_{\text{free}}}{C_{\text{free}}} &\sim 1 + \frac{1}{f_r} \frac{k}{n}. \end{aligned}$$

Since after p traffic signals there is one stop, we can estimate $k/n \sim 1/p$. Then, using (5), yields the following scaling laws:

$$\frac{\langle t \rangle}{T_{\text{free}}} \sim 1 + (1 - \alpha), \quad (10)$$

$$\frac{\langle v \rangle}{V_{\text{free}}} \sim 1 - (1 - \alpha), \quad (11)$$

$$\frac{\langle C \rangle}{C_{\text{free}}} \sim 1 + \frac{2L/\lambda}{f_r} \frac{(1 - \alpha)}{\alpha}. \quad (12)$$

Above resonance ($\alpha > 1$), the period-1 solution is possible if the average time to move between two traffic lights is

$$\langle t \rangle = \frac{L}{v_{\text{wave}}} = T_{\text{free}} \alpha \approx T_{\text{free}} [1 + (\alpha - 1) + \mathcal{O}(\alpha - 1)^2] , \quad (13)$$

and the average velocity is

$$\langle v \rangle = v_{\text{wave}} = \frac{v_{\text{max}}}{\alpha} \approx v_{\text{max}} [1 - (\alpha - 1) + \mathcal{O}(\alpha - 1)^2] . \quad (14)$$

Equations for $\langle t \rangle$, (10) and (13), and for $\langle v \rangle$, (11) and (14), can be combined as

$$\frac{\langle t \rangle}{T_{\text{free}}} = 1 + |1 - \alpha| , \quad (15)$$

$$\frac{\langle v \rangle}{V_{\text{free}}} = 1 - |1 - \alpha| , \quad (16)$$

being symmetrical around resonance.

Symmetric expressions like these cannot be obtained for fuel consumption. In order to estimate fuel consumption above resonance, let us first notice that the trajectory is analogous to Fig. 5. The distance in which rolling friction acts against the engine is

$$x_r = L - \frac{v_{\text{max}}^2 - v_{\text{min}}^2}{2a_-} , \quad (17)$$

and the energy lost when breaking is

$$W_a = \frac{m}{2} (v_{\text{max}}^2 - v_{\text{min}}^2) . \quad (18)$$

Thus, total work between two traffic lights is

$$W = F_r x_r + \frac{m}{2} (v_{\text{max}}^2 - v_{\text{min}}^2) = F_r L + \frac{1}{2} (v_{\text{max}}^2 - v_{\text{min}}^2) \left(m - \frac{F_r}{a_-} \right) . \quad (19)$$

Note that this is equivalent to Eq. (3). In order to obtain v_{min} , we solve the following set of equations:

$$v_0 = v_{\text{min}} \sqrt{1 + \frac{a_+}{a_-}} , \quad (20)$$

$$T = \left(\frac{v_{\text{max}}}{2} - v_{\text{min}} \right) \left(\frac{1}{a_+} + \frac{1}{a_-} \right) + \frac{v_0^2}{2v_{\text{max}} a_+} + \frac{L}{v_{\text{max}}} . \quad (21)$$

These equations follow from Fig. 5. Equation (21) simply states that the time to travel from one light to the next one is equal to $T = L/v_{\text{wave}}$. Thus,

$$\langle C \rangle \sim C_{\text{free}} \left(1 + \frac{2}{f_r} \left[1 - \frac{F_r}{ma_-} \right] \sqrt{\frac{2a_+ a_-}{a_+ + a_-} \frac{L}{v_{\text{wave}}^2} \frac{(\alpha - 1)^{\frac{1}{2}}}{\alpha}} \right) + \mathcal{O}(\alpha - 1) . \quad (22)$$

Fuel consumption behavior is not symmetrical near resonance. This asymmetry is related to the fact that below resonance the car fully stops only once every p signals, whereas above resonance the car never stops, but brakes at every signal. Since C depends strongly on the detailed pattern of acceleration in the trajectory, scalings are different at each side of the resonance. In Fig. 7(b) numerical results, obtained by iterating the map, are plotted, showing good agreement with the approximated expressions Eqs. (12) and (22) (dotted lines). Let us note that f_r is a function of α if we assume that v_{wave} is constant and we vary v_{max} . For $\alpha > 1$ the scaling law we derived above breaks at the period doubling bifurcation, *i.e.*, $\alpha \approx 1.1$ as seen in Fig. 7(b). The strong asymmetry in this figure also suggests that on average, fuel consumption is higher for “impatient” drivers traveling with velocity above the green wave velocity.

The universality of Eq. (16) is also clearly suggested in Fig. 7(a) for the averaged velocity. This is interesting, as the scaling laws have been obtained for equidistant traffic lights, but also hold for varying street length.

Although this critical behavior has been derived for a single car model, we expect it to have an effect when multiple cars (not too many, otherwise they will form a jam) are in the road as well. Indeed, for a single car, it corresponds to traveling a large number of traffic lights without stopping. Since it would keep its maximum velocity during most of the travel, it would not interact with other cars also in the same situation. Then, the critical behavior, in general, would occur when a bundle of cars passes p lights before being stopped, with $p \gg 1$. This is analogous to a system near a phase transition, when the correlation length goes to infinity. We have obtained analytical results for the critical behavior in our simple model, which could then be compared with more complex simulations and measurements.

It is interesting to notice that the scaling relations for velocity and time traveled derived for the green wave strategy can be mapped to the equivalent scaling laws for the $\phi_n = 0$ strategy by rewriting $\alpha \rightarrow 1/\bar{\Omega}$. The actual derivation follows along similar arguments as the ones used for the green wave strategy. For instance the velocity scaling is

$$\frac{\langle v \rangle}{V_{\text{max}}} = 1 - \frac{|1 - \bar{\Omega}|}{\bar{\Omega}}, \quad (23)$$

displayed as the thin line in Fig. 4. In the case of fuel consumption for $\alpha > 1$ (and $\bar{\Omega} < 1$), this mapping is even more evident, since we need to carry the same analysis as above, but with $T = L/v_{\text{wave}} \rightarrow 2\pi/\omega$, *i.e.*, $\alpha \rightarrow 1/\bar{\Omega}$.

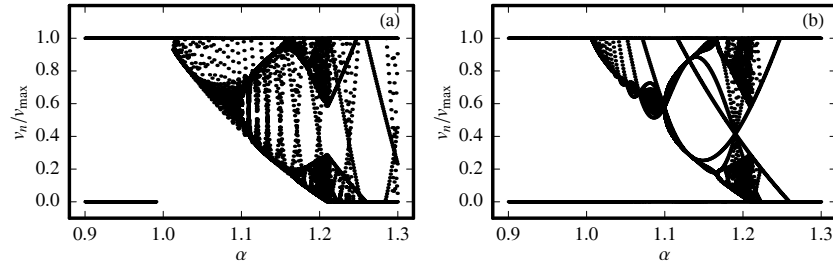


Fig. 8. Bifurcation diagram for the normalized speed v_n/v_{\max} as the control parameter $\alpha = v_{\max}/v_{\text{wave}}$ is varied. Each figure corresponds to a different initial condition: (a) $t_0 = 0$, $v_0 = 0$, and (b) $t_0 = \pi/\omega$, $v_0 = 0$. They contain the transient.

5. Transient Behavior

The results stated in the previous sections regarding resonance and critical behavior for the green wave are valid in the asymptotic regime of the car dynamics. They are valid regardless of the detailed geometry of the system (characterized by the distance L_n between traffic lights). However, trips in cities are typically short, and transient dynamics cannot be neglected in general. In the following sections we intend to describe some features of the transient behavior which may be of interest for city traffic.

Let us consider the green wave strategy. Figure 8 is analogous to Fig. 6(a), but the transient is also shown. In Fig. 8(b) the car starts later. The change in start time is relevant only in the transient part, and of course, both trajectories converge to the same attractor of Fig. 6(a).

Figure 8 shows that, depending on the initial conditions, the evolution can be quite complex, which as mentioned above, may be relevant for city traffic. In particular, strategies for optimizing fuel consumption turn out not to be very obvious even in our simple model. For instance, let us consider the condition $\alpha = 1.3$. The asymptotic solution is a period two orbit with $v_n = 0$ and $v_{n+1} = v_{\max}$ (see Fig. 8). This situation represents a simple case with an interesting asymptotic behavior that may be quite annoying for the drivers. The left panel in Fig. 9 shows v_n/v_{\max} at traffic lights $n = 3$ and $n = 20$ [Figs. 9(a) and 9(b), respectively] for a range of initial conditions in time and velocity. For the same traffic lights we also compute fuel consumption with Eq. (3). This is plotted in the right panel in Fig. 9. Darker (lighter) color represents lower (higher) fuel consumption. Note that these zones are fairly wide and inhomogeneous. Also, there are points associated to high consumption very near to points of low consumption. This result

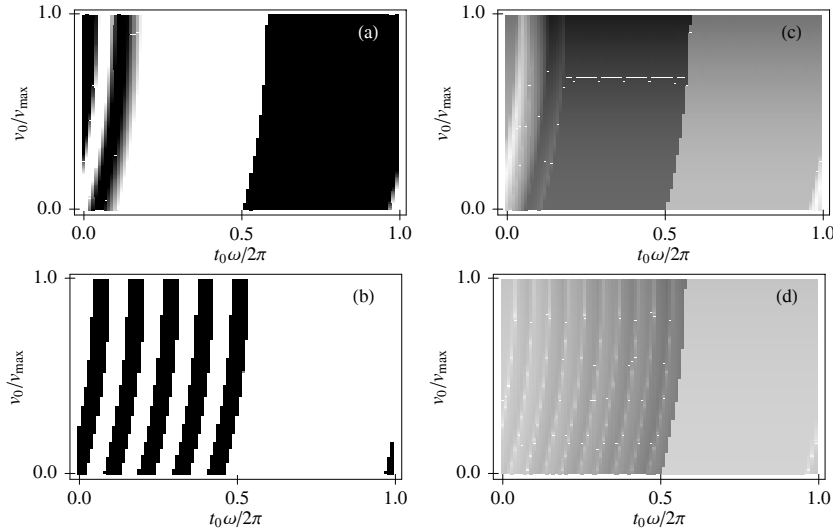


Fig. 9. Transient behavior for $\alpha = 1.3$ according to the initial conditions in the v_0/v_{\max} - $\omega t_0/2\pi$ plane. Lighter tones correspond to higher speeds and higher fuel consumption when crossing the traffic light. In Figs. 9(a) and 9(b), we show the distribution of speed for the third and the twentieth traffic light respectively. In the second column, Figs. 9(c) and 9(d), we show the associated fuel consumption. Fuel consumption is normalized by the maximum fuel consumption among all trajectories analyzed.

points to the difficulty in designing strategies to save fuel or time in city traffic, as optimizations in time traveled may conflict with fuel consumption considerations.

An interesting feature is shown in Fig. 10, for the green wave case, with $\alpha = 1.3$. For two trajectories, the difference in travel time after $n = 20$ traffic

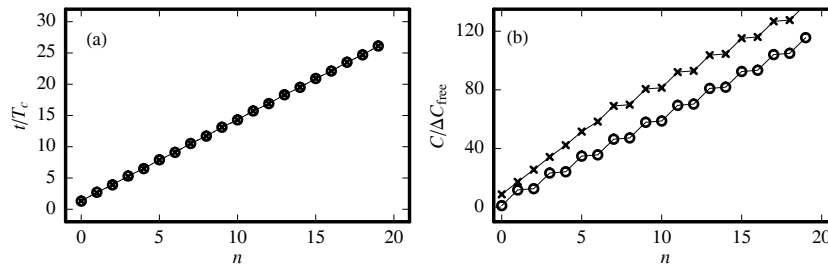


Fig. 10. The comparison of the (a) time traveled (normalized to T_c) and (b) fuel consumption (normalized to $\Delta C_{\text{free}} = F_r L$), for $\alpha = 1.3$, for two particular initial conditions, $v_0 = 18.02$ m/s and $v_0 = 4.55$ m/s, respectively. The rest of the parameters are those for Fig. 6.

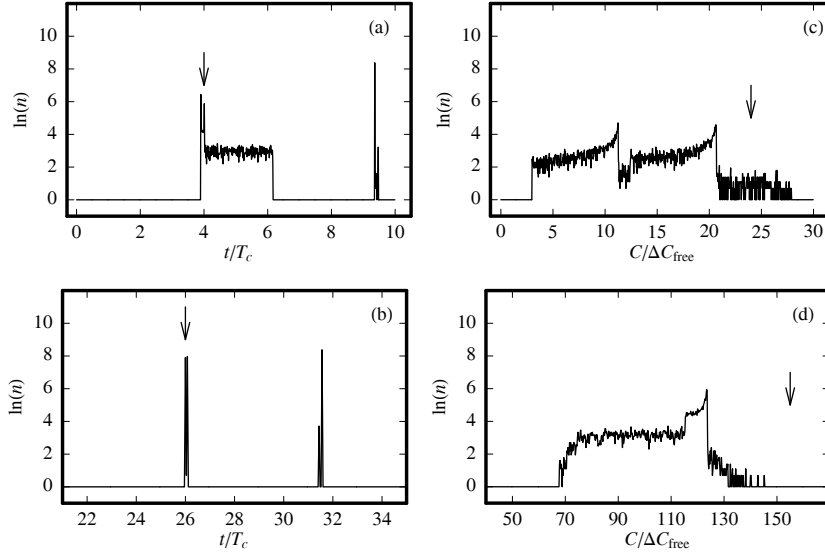


Fig. 11. Transient distributions as measured at different traffic lights for $\alpha = 1.3$, produced by different initial conditions distributed uniformly in the $v_0/v_{\max} - \omega t_0/2\pi$ plane. In Figs. 11(a) and 11(b), we show the distributions of time traveled for the third and the twentieth traffic light respectively. The time has been normalized by T_c . In the second column, Figs. 11(c) and 11(d), we show the associated distribution of fuel consumption. Fuel consumption has been normalized by $\Delta C_{\text{free}} = F_r L$. The vertical arrows are the predictions by the asymptotic formulation given by Eqs. (16) and (22). As expected from Fig. 7(b), the prediction for fuel consumption is not very good for $\alpha = 1.3$.

lights is negligible, whereas they vary by $\sim 20\Delta C_{\text{free}}$ in fuel consumption. These results show that fuel consumption can be a more sensible index to characterize the efficiency of the road system, as compared to travel time, and point out again the difficulty in devising general strategies for traffic control.

Another way to state this is to consider a set of initial conditions distributed uniformly in the $v-t$ plane, and let the trajectories evolve. After $n = 3$ and $n = 20$ traffic lights, the distributions of time and fuel consumption are reconstructed and displayed in Fig. 11 with the same arrangement as in Fig. 9. We note that the distributions are highly asymmetrical and tend to be centered around a certain point that is related to the corresponding asymptotic expression for $\alpha = 1.3$, shown in Fig. 7(a). The width of the distribution for fuel consumption is larger than the width of the distribution for elapsed time, which is consistent with Fig. 10. This shows the high sensitivity of this variable and suggests its relevance in city traffic. On

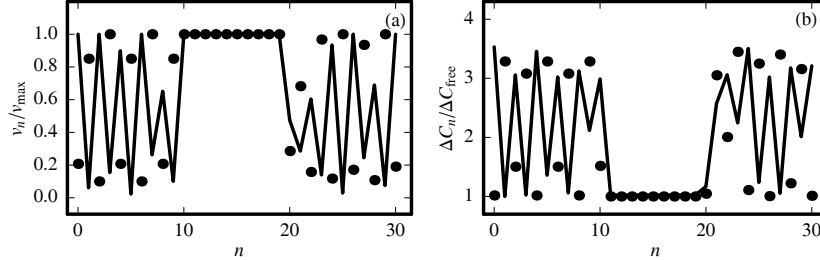


Fig. 12. Orbit collapsing due to the phase change $\phi : 0 \rightarrow \pi$ at the 10th traffic light. In both figures, the period-4 orbit is represented by dots, and the chaotic orbit by a line. (a) Period-4 to free motion and chaos to free motion collapsing, (b) Fuel consumption between lights, ΔC_n , normalized by its minimum value $\Delta C_{\text{free}} = F_r L$.

the other hand, let us remember that in this figure we are representing a statistical distribution, at a given time, of a big number of initial conditions randomly chosen over the whole phase space. The variations that we are seeing here characterize the nontrivial transient part of the trajectories. For the period-2 situation we are considering here, there exist a maximum asymptotic spread in time because of those cars that are caught by a red light during the transient part of the trajectory (remember that the average waiting time at the traffic light is $\sim 2T_c$). Therefore, we can see the convergence of the time distribution to two well defined peaks, whereas for the fuel distribution the two hills shown in Fig. 9(c) will merge into the one observed in Fig. 9(d).

If we are interested in short trips, we may devise strategies that can minimize certain variables by inducing certain transients. For instance let us take $\alpha = 1.19$ where we have a period-4 orbit, and $\alpha = 1.2$ where the orbit is chaotic. However, if at the 10th traffic light the phase is changed from 0 to π , a transition to free resonant motion is observed. This motion eventually collapses back to the period-4 or chaotic orbits respectively [see Fig. 12(a)], but only after going through a nice transient of p traffic lights, which is in close agreement with Eq. (4). As displayed in Fig. 12(b), the phase induced green corridor proposed above reduces fuel consumption because rolling friction is the only source of dissipation. This analysis may suggest another control strategy to improve traffic flow by adaptively changing traffic lights phases. It also gives further insight into the origin of complex solutions when the resonance condition is approached. As time progresses, a periodic or chaotic solution suddenly may spot a green corridor that changes completely its observed trajectory.

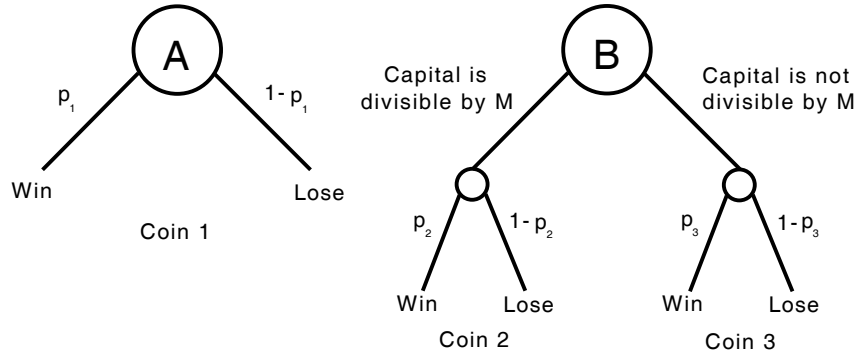


Fig. 13. Realization of a Parrondo game.

6. Parrondo-like Games for Controlling

The phase control of transients, as suggested above, bring us to the concept of treating traffic control as a game. In a game we have a number of agents bounded by a set of rules pursuing a definite goal. In our case, for simplicity, we consider the goal of maximizing the mean velocity, although others goals, such as minimizing fuel consumption, can be considered. Particular attention will be given to the two directional flow, through the same sequence of traffic cars. This problem is interesting, for if we apply the green-wave strategy in a given direction, we may be able to bring the traffic to resonate. But for the cars travelling in the opposite direction, the average speed will be reduced considerably, even compared with the $\phi_n = 0$ (or random) situation (see Fig. 15).

An interesting starting point could be found in the Parrondo's paradox [8], in which two different games are defined so that the player always lose in both of them. But when combined, even in a random sequence, the player wins.

Let's consider the capital gained by a player. Figure 13 shows the decision tree of the standard Parrondo game consisting of only three biased coins, where p_1 , p_2 and p_3 are the winning probabilities for the individual coins. We can define losing games as follow, let us take $\epsilon = 0.005$, then we have $p_1 = 1/2 - \epsilon$ such that the game A is losing in the long run. We play game A by generating a random number $0 \leq r \leq 1$. If $r < p_1$ then we increase our capital by one. Otherwise, we decrease our capital by one. If we play game A continuously, we obtain the curve showing in Fig. 14. For

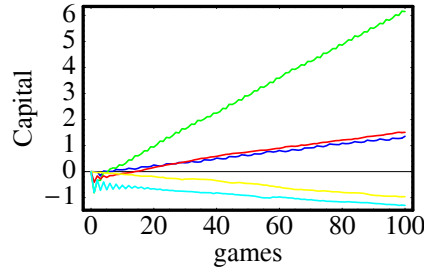


Fig. 14. Five simulations of a 100-game run, with 10,000 trials of each. The two losing games are just A (yellow) and B (cyan). The two moderately winning games are AABBB (blue) and R (red). The big winner is BBABA (green).

the game B, we set $p_2 = 1/10 - \epsilon$, $p_3 = 3/4 - \epsilon$ and $M = 3$. Game B is played by computing if our capital is divisible by M or not. If it is, then we play a game similar to A but with p_2 . If our capital is not divisible by M , then we play a game similar to A but with p_3 . Since the frequency of the coin 3 is higher than the coin 2, game B is also a losing game as shown in Fig. 14.

It is interesting to note that if we now choose a random sequence of game A and B, then we can obtain a winning game, even though A and B are losing games. Furthermore, we can show that certain particular deterministic sequences of games A and B can also produce winning games, as shown in Fig. 14. In particular, the sequence *BBABA* is a very profitable game.

For the traffic problem, we can visualize the car going through the line of randomly distributed traffic lights, as a player flipping a coin to stop or to go through at a give traffic light. Although, is not clear how to perform the original Parrondo’ game in this situation, it is possible to take the basic idea and combine it with a green-wave, which would be our winning game for the traffic going in a particular direction. For the traffic in the opposite direction, the “anti-green-wave” would be the winning strategy. As we now show in Fig. 15, our simulations show interesting results.

In the Fig. 15, we assume a forward “green-wave” strategy which we will perturb in the following way. Let’s take the sequence,

$$\begin{aligned} & \{0, 0, 0, 0\}, 1, \{0, 0, 0\}, 1, \{0, 0, 0, 0, 0\}, 1, \{0, 0, 0, 0, 0, 0\}, 1, \{0, 0, 0\}, 1, \{0, 0, 0, 0\}, 1, \\ & \{0, 0, 0, 0\}, 1, \{0, 0, 0, 0\}, 1, \{0, 0, 0, 0\}, 1, \{0, 0\}, 1, \{0, 0, 0, 0, 0, 0, 0\}, 1, \{0, 0, 0\}, 1, \\ & \{0, 0\}, 1, \{0, 0, 0, 0\}, 1, \{0, 0, 0, 0, 0, 0\}, 1, \{0, 0, 0\}, 1, \{0, 0\}, 1, \{0, 0, 0, 0\}, 1, \\ & \{0, 0\}, 1, \{0, 0, 0, 0, 0\}, 1, \{0, 0\}, 1, \{0, 0, 0, 0, 0\}, \end{aligned}$$

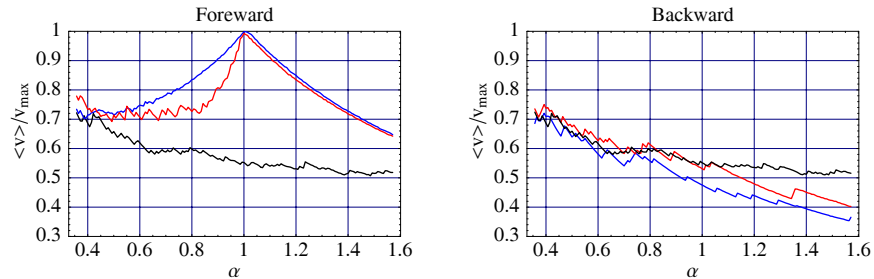


Fig. 15. Normalized average velocity for the cases $\phi_n = 0$ (black), $\phi_n = -\omega x_n / v_{wave}$ (blue) and $\phi_n := \text{game}$ (red). With the game we obtain approximately an 8% of improvement in the backward direction and almost no change in the forward direction (the reference is the green wave strategy at $\alpha = 1$).

where a zero appears when the game is not played, namely we apply the regular forward “green-wave” strategy. If a one appears, then we apply the corresponding forward “green-wave” phase and we add $\Delta\phi = -\omega\left(\frac{2L}{v_{max}} - \frac{v_{max}}{a_-}\right)$. This phase shift, is in favor of the backward direction, by increasing the range of initial conditions that can pass through the traffic light. This is an example of a successful game in this context, as shown in Fig. 15, since it improves on the average velocity for the backward direction, without a considerable reduction in the forward direction.

7. Conclusion

As a complex system, a traffic network has many interesting features. We have developed a minimal model, that consist of a single car going through a sequence of traffic lights, that displays some of the basic features present in city traffic. Even under these simple conditions, we observe a range of complicated behaviors that, for some critical parameters, display non-chaotic motion, chaos and intermittency (not considered here). Hence, certain perturbations may drive the system to a region where the average speed is reduced considerably. We have investigated control procedure through the manipulation of the phase in the traffic light system. We can perform this manipulation deterministically, which can be useful for few cars under very constrained conditions, or statistically, in the spirit of a game, if we maximize the probability of winning most of the time (maximizing the average velocity). This last approach seems to be fruitful given changing conditions in a city. Therefore, the best game (which maximizes the average velocity or minimizes the traveled time) will be dependent on the city conditions and hence spatial and time dependent. This a work in progress.

Appendix: The $M(t, v)$ Map

It is convenient to construct an exact map that relates successive crossing of the traffic lights. Let L be the distance between origin O and next traffic light. After crossing the n^{th} light, the car reaches v_{\max} at

$$\begin{aligned} x_c &= \frac{v_{\max}^2 - v_n^2}{2a_+}, \\ t_c &= t_n + \frac{v_{\max} - v_n}{a_+}, \\ v_c &= v_{\max}, \end{aligned}$$

and continues to move at constant velocity until the decision point

$$\begin{aligned} x_d &= L_n - \frac{v_{\max}^2}{2a_-}, \\ t_d &= t_c + \frac{x_d - x_c}{v_{\max}}, \\ v_d &= v_{\max}. \end{aligned}$$

At this point we have two choices depending on the sign of $\sin(\omega_n t_d + \phi_n)$. If $\sin(\omega_n t_d + \phi_n) > 0$, the car reaches the traffic light with a state

$$\begin{aligned} x_{n+1} &= L_n, \\ t_{n+1} &= t_d + \frac{L_n - x_d}{v_{\max}}, \\ v_{n+1} &= v_{\max}. \end{aligned}$$

If $\sin(\omega_n t_d + \phi_n) < 0$, the car must start slowing down with a_- , and it will take an extra time $\Delta t = v_{\max}/a_-$, to reach the $(n+1)^{\text{th}}$ traffic light and stop. This time must be compared with the next time the light turns green t_g , at which point the car can accelerate again. Defining the phase $\xi_d = \omega_n t_d + \phi_n$, we can compute

$$\xi_g = \omega_n t_g + \phi_n = 2\pi \left(\text{Int} \left[\frac{\xi_d}{2\pi} \right] + 1 \right),$$

where $\text{Int}[x]$ is the integer part of x . Therefore, if $t_d + \Delta t < t_g$, the car will cross the $(n+1)^{\text{th}}$ traffic light with

$$\begin{aligned} x_{n+1} &= L_n \\ t_{n+1} &= t_g, \\ v_{n+1} &= 0. \end{aligned}$$

In the other case, $t_d + \Delta t > t_g$, the car starts accelerating at the state

$$x_g = x_d + v_d(t_g - t_d) - a_-(t_g - t_d)^2/2 ,$$

$$t_g = t_g ,$$

$$v_g = v_d - a_-(t_g - t_d) ,$$

and again we have two cases before it reaches L . We need to determine if the car reaches v_{\max} before the light. We compute the distance at which the car reaches v_{\max} , namely $x_m = x_g + (v_{\max}^2 - v_g^2)/2a_+$. Therefore, if $x_m > L$, then the car reaches the traffic light with

$$x_{n+1} = L_n ,$$

$$t_{n+1} = t_g + \frac{v_{n+1} - v_g}{a_+} ,$$

$$v_{n+1} = \sqrt{v_g^2 + 2a_+(L_n - x_g)} ,$$

otherwise, it reaches v_{\max} at

$$x_m = x_m ,$$

$$t_m = t_g + \frac{v_{\max} - v_g}{a_+} ,$$

$$v_m = v_{\max} ,$$

and the light at

$$x_{n+1} = L_n ,$$

$$t_{n+1} = t_m + \frac{L_n - x_m}{v_{\max}} ,$$

$$v_{n+1} = v_{\max} .$$

References

- [1] A. Benyoussef, H. Chakib, and H. Ez-Zahraouy. *Phys. Rev. E*, 68:026129, 2003.
- [2] G. Boffetta, M. Cencini, M. Falcioni, and A. Vulpiani. *Physics Reports*, 356:367, 2002.
- [3] E. Brockfeld, R. Barlovic, A. Schadschneider, and M. Schreckenberg. *Phys. Rev. E*, 64:056132, 2001.

- [4] R. H. Essenhigh. *Transportation Research*, 8:457, 1974.
- [5] I. Evans. *British J. Appl. Phys.*, 5:187, 1954.
- [6] N. V. Findler and J. Stapp. *Journal of Transportation Engineering*, 118:99110, 1992.
- [7] B. D. Greenshields. *Highway Reserch Board, Proc.*, 14:458, 1935.
- [8] G.P. Harmer and D. Abbott. *Nature (London)*, 402 (6764):864, 1999.
- [9] K. Hasebe, A. Nakayama, and Y. Sugiyama. *Phys. Rev. E*, 68:026102, 2003.
- [10] D. Huang. *Phys. Rev. E*, 68:046112, 2003.
- [11] D. Huang and W. Huang. *Phys. Rev. E*, 67:056124, 2003.
- [12] B. S. Kerner and S. L. Klenov. *Phys. Rev. E*, 68:036130, 2003.
- [13] J. Kuhl, D. Evans, Y. Papelis, R. Romano, and G.S. Watson. *IEEE Computer*, 1995.
- [14] N. Moussa. *Phys. Rev. E*, 68:036127, 2003.
- [15] T. Nagatani. *Phys. Rev. E*, 60:1535, 1999.
- [16] T. Nagatani. *Rep. Prog. Phys.*, 65:1331, 2002.
- [17] T. Nagatani. *Phys. Rev. E*, 68:036107, 2003.
- [18] K. Nagel and M. Paczuski. *Phys. Rev. E*, 51:2909, 1995.
- [19] K. Nishinari, M. Treiber, and D. Helbing. *Phys. Rev. E*, 68:067101, 2003.
- [20] J. B. Rundle, K. F. Tiampo, W. Klein, and J. S. Martins. *Proc Natl Acad Sci*, 67:2514, 2002.
- [21] G. Stachowiak and A. W. Batchlor. *Engineering Tribology*. Butterworth-Heinemann, 2001.
- [22] B. A. Toledo, E. Cerda, V. Muñoz, J. Rogan, R. Zarama, and J. A. Valdivia. *Phys. Rev. E*, 75:026108, 2007.
- [23] B. A. Toledo, V. Muñoz, J. Rogan, C. Tenreiro, and J. A. Valdivia. *Phys. Rev. E*, 70:016107, 2004.
- [24] M. Treiber and D. Helbing. *Phys. Rev. E*, 68:046119, 2003.